water

MDPI

Article

The Thresholds of Sediment-Generating Rainfall from Hillslope to Watershed Scales in the Loess Plateau, China

Yue Liang [1,2], Juying Jiao [1,3,*], Weiqin Dang [4] and Wei Cao [4]

1 State Key Laboratory of Soil Erosion and Dryland Farming on the Loess Plateau, Institute of Soil and Water Conservation, Academy of Sciences and Ministry of Water Resources, 26 Xinong Road, Yangling, Xianyang 712100, China; ly8868130@163.com
2 University of Chinese Academy of Sciences, Beijing 100049, China
3 Institute of Soil and Water Conservation, Northwest A & F University, 26 Xinong Road, Yangling, Xianyang 712100, China
4 Suide Station for Soil and Water Conservation Research, Management Committee of Yellow River Water Conservancy, Yulin 719000, China; dangwq@163.com (W.D.); hhcaowei@126.com (W.C.)
* Correspondence: jyjiao@ms.iswc.ac.cn

Received: 17 September 2019; Accepted: 11 November 2019; Published: 14 November 2019

Abstract: Obtaining practical thresholds for erosive rainfall plays a crucial role in calculating rainfall erosivity and predicting water erosion. Nevertheless, the study of thresholds on subwatershed and watershed scales remains scarce. Given this, we presented the critical rainfall that generated the outflows of subwatersheds and watersheds as the threshold of sediment-generating rainfall. On the basis of the observation of twelve nested topographical units at the Peijiamaogou watershed in the Loess Plateau of China, we fitted regression relationships between rainfall indexes (rainfall amount, maximum 30-min intensity, maximum 60-min intensity, rainfall amount multiply maximum 30-min intensity, and rainfall amount multiply maximum 60-min intensity) and the proportion of cumulative sediment yield to the total sediment yield. We determined the thresholds of sediment-generating rainfall and explored the variabilities of thresholds across different spatial scales. Moreover, the covering area proportion (CAP) with rainfall indexes higher than the thresholds was also employed as thresholds at the subwatershed and watershed scales. The thresholds of CAP for P and I_{30} were 50.5% and 47.6% at the subwatershed scale, while 31.0% and 30.3% at the watershed scale. The thresholds of P and I_{30} at the subwatershed scale were higher than those of hillslope scale, while the threshold of I_{30} at the watershed scale was smaller compared to the other scales. In general, I_{30} was viewed as the best threshold among single rainfall indexes across different spatial scales, while P was not recommended as a practical threshold. This study can improve the prediction accuracy of water erosion across different spatial scales and develop the spatial scale effect of sediment yield in the loess hilly areas.

Keywords: soil erosion; sediment yield; rainfall erosivity; spatial scales

1. Introduction

Soil erosion has been a widely recognized eco-environmental problem worldwide [1]. It not only results in land degradation by reducing soil fertility and soil organic carbon content [2–4], but also leads to off-site siltation of reservoirs or lakes and water eutrophication downstream [5,6]. Rainfall is acknowledged as the primary driving factor of soil erosion, and its potential ability to trigger soil erosion is known as rainfall erosivity [7,8]. However, not all rainfall events bring on soil erosion [8–10].

The critical rainfall value that distinguishes the erosive and non-erosive rainfall is known as the threshold of erosive rainfall [8,11,12].

The calculation of rainfall erosivity is challenging, and thus rainfall events that do not cause erosion should be neglected to effectively save processing time [8,11,12]. Hence, it is of vital importance to determine the thresholds of erosive rainfall in calculating rainfall erosivity and predicting soil erosion. As a consequence, the thresholds, as well as the characteristics of erosive rainfall, have been studied widely by previous researchers [8,11–14]. Wischmeier et al. [12] proposed 12.7 mm as the threshold of erosion rainfall amount. This threshold value has been employed in the Universal Soil Loss Equation (USLE), Revised Universal Soil Loss Equation (RUSLE), and other researches for calculating rainfall erosivity worldwide [15,16]. It has been proven that the thresholds of erosive rainfall could be affected by land use types, agrotype, and topography. Xia et al. [11] found that the thresholds of erosive rainfall under vegetation were higher than those of bareland and farmland. The underlying surface with soil and water conservation measures was also demonstrated to effectively raise the thresholds of erosive rainfall [13]. Additionally, the thresholds of erosive rainfall decrease dramatically with increasing gradient [17].

As has been documented, the thresholds of erosive rainfall based on the data of runoff plots should probably not be extrapolated directly to the watershed scale [8,11] because of the spatial scale effect of erosion processes and sediment production [18–25]. The erosive rainfall events which cause soil erosion at the hillslopes do not always lead to outflows of subwatersheds or watersheds. As a consequence, we call the rainfall events which result in outflows of subwatersheds or watersheds sediment-generating rainfall. The practical threshold to distinguish whether a rainfall event belongs to rainfall event which generated sediment is referred to as the threshold of sediment-generating rainfall. The thresholds include rainfall amount, rainfall intensities, rainfall durations, and their combination indexes.

Obtaining thresholds of sediment-generating rainfall across different spatial scales plays a crucial role in calculating rainfall erosivity and forecasting soil erosion and sediment yield from hillslope to watershed scales. Xie et al. [8] compared the thresholds of hillslopes (0.09–1.72 hm^2) and a small agro-watershed (18 hm^2), indicating that thresholds of sediment-generating rainfall for amount and average intensity in the hillslopes are 1.6 and 1.5 times higher than those of the larger watershed, respectively. Liang et al. [26] determined the thresholds of sediment-generating rainfall for 20 watersheds in the Loess Plateau and demonstrated that the thresholds of amount ranged from 7.5 to 33.5 mm due to different underlying surface conditions and area size. However, integrated research on determining the thresholds of sediment-generating rainfall across different spatial scales remains scarce.

Peijiamaogou watershed is a typical agro-watershed on the hilly and gully region of the Loess Plateau, where the rainfall and sediment in different spatial scales have been measured for several decades and mass data of rainfall and sediment were collected. In this study, we analyzed the data of rainfall characteristics and specific sediment yield of twelve instrumented nested landscape units from 1990 to 2010, including eight runoff plots with area from 38.8 to 1024 m^2, three subwatersheds (0.069 to 0.45 km^2), and Peijiamaogou watershed (39.3 km^2). The present study has three specific objectives: (1) To obtain the thresholds of sediment-generating rainfall from hillslope to watershed scale; (2) to evaluate the thresholds of sediment-generating rainfall and determine the best rainfall indexes regarding different spatial scales; (3) to reveal the variance of thresholds across spatial scales. This study could provide a reference for calculating rainfall erosivity and improving the prediction accuracy of sediment yield across different spatial scales, additionally, having theoretical significance in developing the spatial scale effect theory of sediment yield in the loess hilly areas.

2. Materials and Methods

2.1. Study Area

Peijiamaogou watershed (110°17–110°23′ E, 37°28′–37°33′ N), a typical unmanaged watershed, is located in the hilly and gully region of the Loess Plateau. The watershed covers a drainage area of

39.3 km^2 with channel gradient of 1.22%. The main channel length is about 11 km with gully density of 2.69 km km^{-2}, and elevations ranging from 789 to 1122 m. The area of inter-gully and gully land account for 49.1% and 50.9% of the total area in the watershed, respectively [27,28]. The region of the watershed is mainly composed of some farmland, natural slopes, bareland, steep cliffs, villages, roads, and ditch beds. The vegetation in this watershed is sparse and mostly distributed on the fallow slopes. The soil of the original landscape exhibits a fine-silty texture with 32.1%, 60.5%, and 7.5% of sand, silt, and clay contents, respectively [29]. There are sporadic soil and water conservation measures in the Peijiamaogou watershed [30]. There were almost no check dams or reservoirs in the watershed. Annual average precipitation was 307.7 mm from 1986 to 2010; moreover, about 73% of the precipitation was concentrated between June and September. The annual runoff volume varied from 0.12×10^6 to 6.0×10^6 m^3 between 1986 to 2010, with an average value of 1.01×10^6 m^3. The annual sediment yield varied from 7.63 to 2.58×10^4 t km^{-2} with significant inter-annual variability from 1986 to 2008 [31]. There are many subwatersheds dissected by dense channel networks in the watershed. Generally, the subwatersheds are without base-flow discharges and typically smaller than 1 km^2 in size, while the area of watersheds are typically higher than 1 km^2 [32].

2.2. Data Source

Measurements of rainfall characteristics (amount, duration, and intensity), total runoff, suspended sediment concentration, and sediment yield in twelve geomorphic units were managed by the stream-gauging staff of the Yellow River Conservancy Commission (YRCC) since 1986 according to the national standards [31]. The data of rainfall and sediment for the Peijiamaogou watershed, the Qiaogou subwatershed (a branch of the Peijiamaogou watershed), and No. 1 branch, No. 2 branch, eight embedded runoff plots in the Qiaogou subwatershed from 1990 to 2010 were selected to obtain the thresholds of sediment-generating rainfall (Tables 1 and 2). The runoff of the subwatersheds and the watershed were recorded by flumes, which were constructed at the outlets of the watershed and the subwatersheds, while the runoff of field runoff plots were measured by the water tanks. Suspended sediment concentration was measured from the runoff samples, and specific sediment yield equalled the runoff volume multiplied by respective suspended sediment concentration.

Table 1. Characteristics of the instrumented plots [31].

Plot No.	Geomorphic Unit	A (m^2)	L (m)	S (°)	No. of Rainfall Events	No. of Runoff Events	Specific Sediment Yield (t km^{-2})
1	The upper hillslope 1	38.8	19.4	18.0	701	48	414.9 ± 69.3
2	The upper hillslope 2	97.0	19.4	18.0	701	49	664.9 ± 132.9
3	The upper hillslope 3	194	19.4	18.0	701	50	586.7 ± 118.5
4	The lower hillslope	181	18.1	23.9	701	50	751.5 ± 160.7
5	Hillslope	456	45.6	22.0	701	50	667.5 ± 132.8
6	Whole slope	2492	98.9	32.3	701	52	1961.2 ± 430.0
7	Gully-slope 1	1584	55.6	39.0	701	45	651.6 ± 152.7
8	Gully-slope 2	1024	53.0	40.1	701	41	1215.0 ± 367.8

L represents the plot length, S represents the mean slope, A represents the area; data of the average specific sediment yield are given as means ± standard error of means.

There are six precipitation stations in the Qiaogou subwatershed and seven primary precipitation stations in the Peijiamaogou watershed. All runoff plots share one precipitation station in the Qiaogou subwatershed (Figure 1). The rainfall data were recorded continuously using self-recording rain gauges. If the interval was less than 6 h between two consecutive rainy periods, then the two periods were regarded as one rainfall event [12,33]. For every precipitation station, data of rainfall amount, duration, and maximum intensities for every rainfall event were extracted and calculated. The characteristics of the instrumented runoff plots and gauging stations are listed in Table 1, Table 2 and Figure 1.

Table 2. Characteristics of the gauging stations [31].

Location	Scale	Gauging Station	Control Area (km^2)	Channel Length (m)	No. of Rainfall Events	No. of Runoff Events	Average Specific Sediment Yield (t km^{-2})
Qiaogou	Subwatershed	No. 1 branch	0.069	869	701	59	1233.4 ± 237.2
		No. 2 branch	0.093	805	701	60	1563.1 ± 464.7
		Qiaogou	0.45	1400	701	64	1196.9 ± 395.8
Peijiamao	Watershed	Peijiamaogou	39.3	11,000	706	72	2201.1 ± 79.6

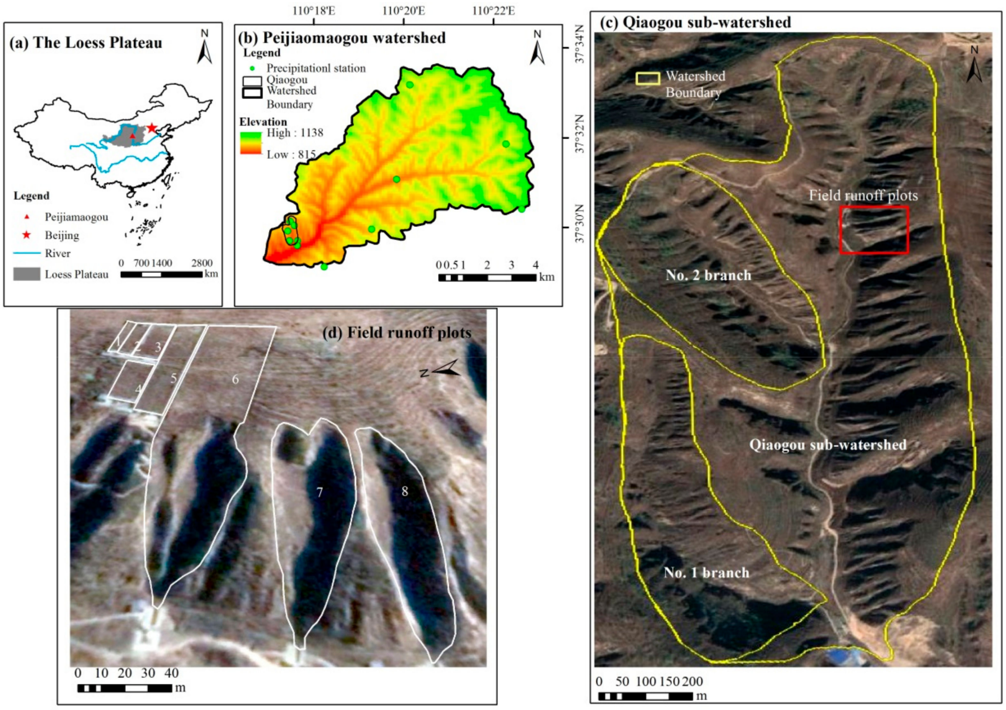

Figure 1. Location of the study area (The Loess Plateau (**a**), the Peijiamaogou watershed (**b**), the Qiaogou subwatershed (**c**), field runoff plots in the Qiaogou subwatershed (**d**)). Note: The numbers are the same to those in Table 1.

Conventionally, the term "soil erosion" is applied to hillslopes, and the term "sediment yield" is used for a watershed or river system. For convenience, we used specific sediment yield (SSY, t·km^{-2}) to represent both cases hereafter. It should be noted that the SSY data refer to suspended load only.

2.3. Statistical Analysis

2.3.1. The Calculation of Thresholds for Sediment-Generating Rainfall

Among rainfall maximum intensities, the maximum 30-min intensity (I_{30}) and maximum 60-min intensity (I_{60}) are well correlated with soil loss [34] and are often implemented to calculate rainfall erosivity [7,11,35]. Hence, we choose rainfall amount (P, mm), maximum 30-min intensity (I_{30}, mm min^{-1}), maximum 60-min intensity (I_{60}, mm min^{-1}), and their recombination indexes (rainfall amount multiply maximum 30-min intensity (PI_{30}, mm^2 min^{-1}), rainfall amount multiply maximum 60-min intensity (PI_{60}, mm^2 min^{-1})) to calculate the thresholds of sediment-generating rainfall. In the Qiaogou subwatershed and the Peijiamaogou watershed, the rainfall indexes used the mean values of the subwatershed and the watershed, which were calculated with the Theisen polygon method [36].

The calculation of the thresholds of sediment-generating rainfall was accomplished as follows [8,14]: (1) All the runoff events were arranged in descending order of rainfall amount, along with associated SSY of a plot or watershed. (2) Sum the cumulative SSY in descending order of rainfall amount, as well as calculating the cumulative percentage of SSY to overall SSY of all runoff events. (3) A regression equation of rainfall amount and associated cumulative percentage of SSY was obtained by selecting the maximal R^2 of the regression equation. (4) Given a cumulative percentage of SSY, a threshold of sediment-generating rainfall was determined [8]. In this study, the cumulative percentage value that we applied was 95%, because 5% of the total soil loss can be allowable in the Loess Plateau [14]. Rainfall events with rainfall amount above the threshold were considered as sediment-generating rainfall [8]. The same process was used to obtain thresholds of the other rainfall indexes (I_{30}, I_{60}, PI_{30}, PI_{60}).

2.3.2. Thresholds of Rainfall Covering Area Proportion (CAP)

In the watersheds, the thresholds were calculated by mean values of rainfall indexes under each rainfall event, which could not fully represent the detailed rainfall characteristics in the whole watershed. Thus, we presented the thresholds of covering area proportion (CAP) as the thresholds of sediment-generating rainfall at the subwatershed and watershed scales. CAP means the ratio of the covering area, in which the values of rainfall indexes at the event time scale are higher than their respective values of thresholds for the whole watershed, to the watershed area. It is advisable to apply the thresholds of CAP for watersheds because of the high rainfall spatial heterogeneity at the event time scale in the Loess Plateau [34,37]. Detailed procedures for determining the thresholds are as follows: (1) Calculate the CAP for each rainfall event using the "Theisen polygon method": Divide the watershed into several units consisting of one precipitation station by the "Theisen polygon method", then the rainfall indexes of each precipitation station are used to represent those of respective units; the CAP is the area proportion of units with the rainfall indexes higher than the thresholds of the watershed. (2) Determine the thresholds of CAP using the method for calculating the other thresholds of rainfall indexes mentioned above.

2.3.3. Thresholds Under Different Rainfall Types

Because of the significant discrepancies in soil erosion under different rainfall types, we used the rainfall concentration index (*CI*) to classify rainfall events [34,38]. *CI* is defined as:

$$CI = P_{60}/P \tag{1}$$

where *CI* represents the concentration index of a rainfall event (%), P_{60} is the maximum 60-min rainfall amount of a given rainfall event (mm), and *P* is the total rainfall amount of the rainfall event (mm).

The rainfall types were classified depending on the *CI*. When $CI \geq 80\%$, the rainfall events were determined as rainfall type A, while $20\% < CI < 80\%$, the rainfall events were determined as rainfall type B, and the rainfall events with $CI \leq 20\%$ were determined as rainfall type C.

In the Peijiamaogou watershed, the runoff events of type A and B occurred 23 and 44 times during the experimental period, respectively. However, there were only five rainfall events of type C which generated sediment in the study period. This number is too small to calculate the thresholds and thus, the thresholds were determined based on rainfall events under rainfall types A and B.

2.3.4. The Evaluation of Thresholds

To evaluate the rationality for thresholds of sediment-generating rainfall, we presented the mixing index (MI) [8]. A better threshold can be obtained with smaller MI.

The mixing index was defined as follow:

$$\mathrm{MI} = \frac{\mathrm{N_{up}} + \mathrm{N_{dn}}}{\mathrm{N_t}} \times 100\% \tag{2}$$

where MI = mixing index, representing the rate of the number of events that were "misclassified" in the rainfall events which generated sediment or not to the number of total rainfall events; $\mathrm{N_{up}}$ = number of rainfall events which did not generate sediment with characteristics higher than the thresholds; $\mathrm{N_{dn}}$ =

number of rainfall events which generated sediment with characteristics smaller than the thresholds generating sediment; and N_t = total number of rainfall events.

In addition, N_{up}/N_t implies the proportion of rainfall events which did not generate sediment in calculation of rainfall erosivity; N_{dn}/N_t represents the rate of sediment generating events which were missed in the calculation of rainfall erosivity to all rainfall events.

3. Results

3.1. Thresholds of Sediment-Generating Rainfall

The P for thresholds of sediment-generating rainfall on the hillslope runoff plots were essentially constant, with an average value of 14.0 mm (Table 3). The P for thresholds of two gully slopes were 15.5 and 15.2 mm, respectively. Additionally, the thresholds of No. 1 branch, No. 2 branch, the Qiaogou subwatershed and the Peijiamaogou watershed were higher than those of hillslopes. The average thresholds of maximum rainfall intensities and the recombination indexes for the subwatersheds were higher than those for runoff plots on hillslopes (Table 3). However, the thresholds of I_{30} and I_{60} for the Peijiamaogou watershed were smaller than those for other spatial scales.

The thresholds of maximum rainfall intensities had an improved effectiveness for separating sediment-generating rainfall compared to the thresholds of rainfall amount and recombination indexes. The MIs using the thresholds of P were 11.8 to 14.1%, which were far higher compared to the thresholds of maximum rainfall intensities and recombination indexes. Among all spatial scales, N_{up}/N_t were much higher than those of N_{dn}/N_t. The rates of N_{up} to N_t for runoff plots were higher compared to the subwatersheds and the watershed, whereas the N_{dn}/N_t of runoff plots were smaller than those of the subwatersheds and the watershed. The values of MI and N_{up}/N_t for thresholds of maximum rainfall intensities were much smaller compared to the thresholds of rainfall amount and recombination indexes (Figure 2). Hence, the thresholds of I_{30} were recommended to employ in different spatial scales with an average MI of 4.2% (Figure 2).

Table 3. Thresholds of sediment-generating rainfall across different spatial scales.

Spatial Scale	Geomorphic Unit	P	I_{30}/(mm·min^{-1})	I_{60}/(mm·min^{-1})	PI_{30}/(mm^2·min^{-1})	PI_{60}/(mm^2·min^{-1})
Plot scale	The upper hillslope 1	13.8	0.23	0.18	4.11	3.19
	The upper hillslope 2	14.1	0.24	0.18	4.29	3.35
	The upper hillslope 3	14.1	0.23	0.19	4.17	3.26
	The lower hillslope	13.9	0.24	0.20	4.50	3.56
	Hillslope	14.1	0.22	0.19	4.00	3.29
	Gully-slope 1	14.2	0.26	0.20	4.06	3.32
	Gully-slope 2	15.2	0.26	0.21	4.51	3.49
	Whole slope	14.0	0.23	0.19	3.39	2.83
	Plot average	14.2	0.24	0.19	4.13	3.29
Subwatershed scale	No. 1 branch	14.3	0.25	0.19	4.13	3.14
	No. 2 branch	15.3	0.29	0.23	5.92	4.02
	Qiaogou	15.6	0.27	0.21	5.06	3.62
	Subwatershed average	15.1	0.27	0.21	5.04	3.59
Watershed scale	Peijiamaogou	15.9	0.20	0.16	4.35	3.49

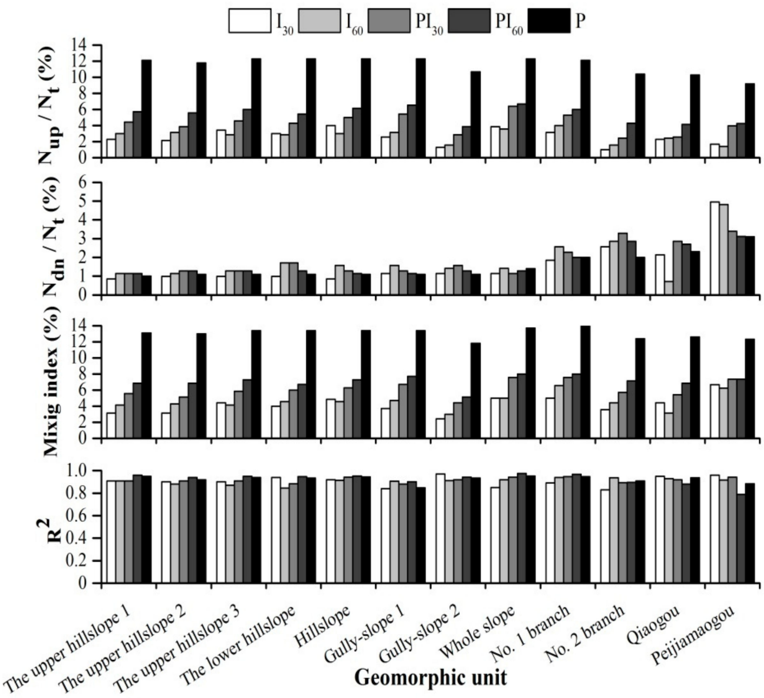

Figure 2. The mixing indexes and R^2 of regression equation for thresholds (P, I_{30}, I_{60}, PI_{30}, PI_{60}) across different spatial scales.

In sum, 0.24, 0.27, and 0.20 mm min^{-1} of I_{30} were supposed to the thresholds for the hillslope, subwatershed, and watershed scales, respectively.

3.2. Thresholds of Covering Area Proportion (CAP)

To analyze the thresholds of CAP, we decided to obtain the CAP of P I_{30} and PI_{30} to determine the thresholds in the Qiaogou subwatershed and the Peijiamaogou watershed. Table 4 indicates that the thresholds of CAP had a greater applicability in the Qiaogou and Peijiamogou watersheds than other thresholds with smaller MIs. For instance, the MIs of CAP thresholds for I_{30} were 3.4 and 4.4%, respectively, and these values were smaller than MIs of thresholds for I_{30} in Qiaogou (4.4%) and Peijiamogou (6.7%) (Table 4, Figure 2). Accordingly, the CAP could represent thresholds of sediment-generating rainfall in the subwatershed and the watershed scales. Among all rainfall indexes of CAP, I_{30} exhibited the least MIs in the subwatershed and the watershed, followed by the PI_{30}, whereas P showed much larger MIs compared to I_{30} and PI_{30} (Table 4). Generally, the applied I_{30} threshold of CAP exceeding 0.27 mm min^{-1} would be 48% at the subwatershed scale and those exceeding 0.20 mm min^{-1} would be 30% at the watershed scale, respectively.

Table 4. Thresholds of covering area proportion (CAP) and their evaluations in the subwatershed and the watershed (%).

Precipitation Station	Index	CAP/(%)	$\frac{N_{up}}{N_t}$/%	$\frac{N_{dn}}{N_t}$/%	MI/%
Qiaogou	$P > 15.6$ mm	50.5	8.1	2.4	10.6
	$I_{30} > 0.27$ mm·min^{-1}	47.6	1.0	2.4	3.4
	$PI_{30} > 5.14$ mm^2·min^{-1}	47.4	2.1	3.0	5.1
Peijiamaogou	$P > 15.9$ mm	31.0	7.8	2.7	10.5
	$I_{30} > 0.20$ mm·min^{-1}	30.3	2.1	2.3	4.4
	$PI_{30} > 4.35$ mm^2·min^{-1}	26.2	3.5	2.4	5.9

3.3. Thresholds of Sediment-Generating Rainfall under Different Rainfall Types

There were considerable differences in the thresholds under two rainfall types (Table 5). The thresholds of P under rainfall type B for different spatial scales were higher than those of rainfall type A (Table 5). The variation of thresholds among different spatial scales was inconsistent under different rainfall types. The results obviously demonstrate that all of the thresholds in the subwatersheds and the watershed were higher than those of runoff plots under rainfall type A. As for rainfall type B, the thresholds in the subwatersheds and the watershed were smaller than those of runoff plots except for thresholds of I_{30} in the Qiaogou subwatershed. Additionally, thresholds of I_{30} under rainfall type B were higher than those under rainfall type A in runoff plots, but smaller in the subwatersheds and the watershed.

Table 5. The thresholds of sediment-generating rainfall under rainfall types A and B.

Spatial Scale	Site	A			B		
		P/mm	I_{30}/(mm·min^{-1})	PI_{30}/(mm^2·min^{-1})	P/mm	I_{30}/(mm·min^{-1})	PI_{30}/(mm^2·min^{-1})
Plot scale	The upper hillslope 1	9.3	0.24	2.30	24.5	0.28	6.85
	The upper hillslope 2	9.3	0.24	2.42	25.7	0.27	7.48
	The upper hillslope 3	9.3	0.21	2.25	24.9	0.26	6.98
	The lower hillslope	9.5	0.24	2.44	27.5	0.26	7.73
	Hillslope	10.1	0.23	2.75	25.1	0.28	7.26
	Gully-slope 1	9.0	0.23	2.39	27.2	0.27	6.47
	Gully-slope 2	8.8	0.23	2.18	27.8	0.27	8.91
	Whole slope	10.2	0.23	2.36	27.4	0.23	5.80
	Plot average	9.4	0.23	2.39	26.3	0.27	7.19
Subwatershed scale	No. 1 branch	13.5	0.33	5.35	20.2	0.18	4.28
	No. 2 branch	15.8	0.40	6.09	22.9	0.20	4.73
	Qiaogou	12.6	0.32	4.21	21.6	0.25	5.19
	Subwatershed average	14.0	0.35	5.22	21.6	0.21	4.73
Watershed scale	Peijiamaogou	12.1	0.25	2.79	21.4	0.20	5.46

Among the thresholds of different rainfall indexes, the MIs of the thresholds for I_{30} were less compared to those of P and PI_{30} (Figure 3). Thus, it was better to employ the I_{30} as thresholds of sediment-generating rainfall under rainfall types A and B. In general, we recommend using I_{30} values of 0.23, 0.35, and 0.25 mm min^{-1} (Table 5) as thresholds at the hillslope, subwatershed, and watershed scales under rainfall type A, and I_{30} values of 0.27, 0.21, and 0.20 mm min^{-1} as thresholds at the hillslope, subwatershed, and watershed scales under rainfall type B.

Generally, thresholds of CAP exceeding rainfall thresholds for P, I_{30}, and PI_{30} of the Qiaogou subwatershed were higher than those of the Peijiamaogou watershed. Thresholds of CAP for P and PI_{30} under rainfall type B were higher than those under rainfall type A. While for I_{30}, the thresholds of those under rainfall type B were smaller than those under rainfall type A (Table 6). For rainfall type A, CAPs of I_{30} are recommended for use as the thresholds of sediment-generating rainfall with smaller average MIs (3.3%). As for rainfall type B, the CAPs for PI_{30} had better effectiveness compared to other rainfall indexes.

In general, we concluded that the CAP exceeding rainfall thresholds for I_{30} and PI_{30} should be employed as thresholds of CAP at the subwatershed and watershed scales under rainfall types A and B, respectively. In practice, thresholds of CAP regarding I_{30} would be 68.3% and 16.4%, respectively, at the subwatershed and watershed scales under rainfall type A, and that regarding PI_{30} would be 54.9% and 31.9%, respectively, at the subwatershed and watershed scales under rainfall type B, respectively (Table 6).

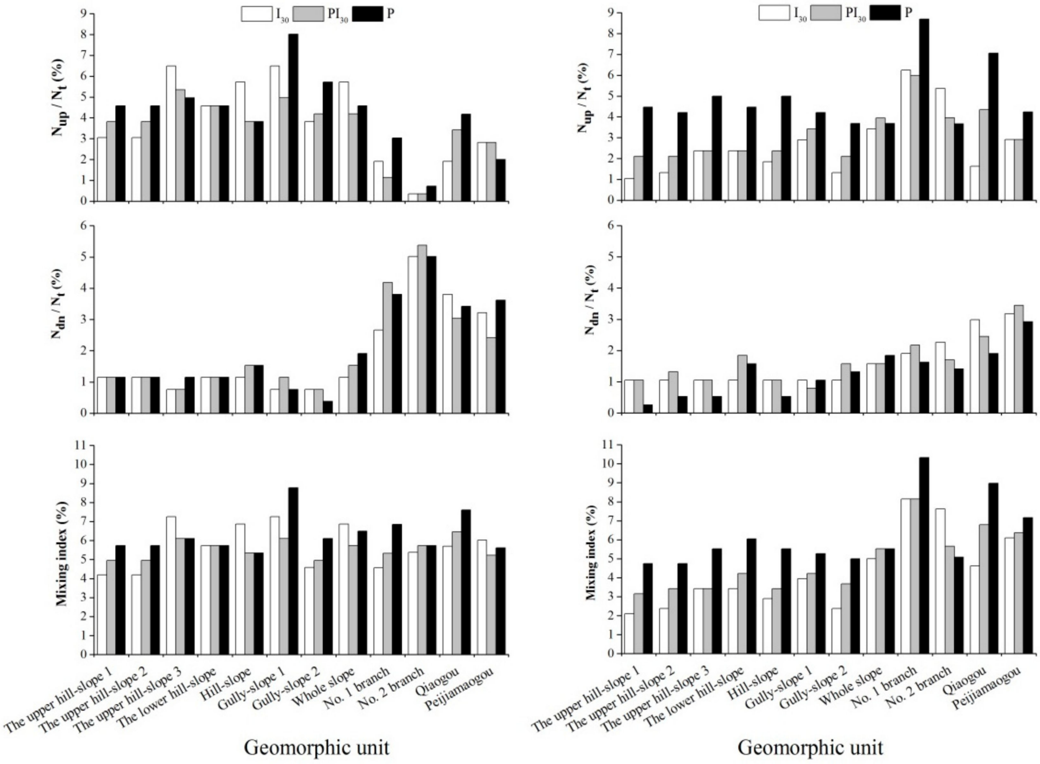

(**a**) (**b**)

Figure 3. The evaluation for thresholds of sediment-generating rainfall under rainfall type A (**a**) and B (**b**).

Table 6. Thresholds of cover area proportion (CAP) and their evaluations in the Qiaogou and Peijiamaogou watersheds under rainfall types A and B.

Precipitation Station	Rainfall Type	Index	CAP/(%)	$\frac{N_{up}}{N_t}$/%	$\frac{N_{dn}}{N_t}$/%	MI/%
Qiaogou	A	$P > 12.6$ mm	20.0	1.9	5.3	7.2
		$I_{30} > 0.34$ mm·min^{-1}	68.3	0.8	2.3	3.0
		$PI_{30} > 4.01$ mm^2·min^{-1}	27.8	0.8	4.6	5.3
	B	$P > 21.6$ mm	83.0	4.6	0.8	5.4
		$I_{30} > 0.25$ mm·min^{-1}	41.2	1.9	3.3	5.2
		$PI_{30} > 5.19$ mm^2·min^{-1}	54.9	2.4	2.7	5.2
Peijiamaogou	A	$P > 12.1$ mm	9.6	1.6	3.2	4.8
		$I_{30} > 0.25$ mm·min^{-1}	46.4	1.6	2.0	3.6
		$PI_{30} > 2.79$ mm^2·min^{-1}	29.3	2.0	2.8	4.8
	B	$P > 21.4$ mm	67.3	4.0	2.9	6.9
		$I_{30} > 0.20$ mm·min^{-1}	32.4	2.7	3.4	6.1
		$PI_{30} > 5.46$ mm^2·min^{-1}	31.9	2.7	2.7	5.3

4. Discussion

4.1. The Thresholds of Sediment-Generating Rainfall Under Different Rainfall Types

We divided rainfall events which generated sediment into three rainfall types based on rainfall concentration index and determined thresholds under rainfall types A and B [34]. The rainfall type A, with high intensity and short duration, occurred from severe convective weather and was considered to cause most of the erosive rainfall events and a large proportion of runoff and soil erosion [38,39]. The high rainfall intensity resulted in forming a surface crust and sealing which accelerated surface flow [38], reducing infiltration rate and generating surface flow rapidly [40–43]. Moreover, sediment transport capacity of overland flow increased with the rising of rainfall intensity [44]. The time to runoff of high-intensity rainfalls also declined compared to low-intensity rainfalls under simulation experiments [45]. Accordingly, the events of rainfall type A with less rainfall amount could generate runoff because of the higher rainfall intensity compared to rainfall type B. In turn, rainfall with weak rainfall intensity and long duration led to improved infiltration and induced less erosive rainfall events [38,39,44]. Therefore, thresholds of P for rainfall type B were higher than those of rainfall type A under different spatial scales.

Wang and Jiao [34] demonstrated that the spatial heterogeneity of rainfall amount under type A was higher compared to that under rainfall type B in watersheds. In most circumstances, the area of rainfall center of rainfall events under rainfall type A was only several square kilometers [34]. Consequently, the maximum value of P of a rainfall event under rainfall type A at the subwatershed and watershed scales would be higher than that of a rainfall event with the same mean rainfall amount under rainfall type B. Moreover, the thresholds of P (14.3–15.3 mm) of the subwatersheds (No. 1 and 2 branches) were smaller than those of the Peijiamaogou watershed (15.9 mm) and the Qiaogou subwatershed (15.6 mm) (Table 3). In a rainfall event under rainfall type A, rainfall amount of partial region in the watershed would be higher than the amount thresholds at the subwatershed or watershed scales, while the rainfall amount of other regions was not. In the partial region, the rainfall amount was much higher than the inner subwatersheds (for instance, No. 1 and 2 branches) and runoff would be probably generated rapidly and transport the sediment to the outlets of the subwatershed and the watershed. Furthermore, there was a large area of sloping cropland, bareland, villages, and roads, which were susceptible to soil erosion in the Peijiamogou watershed [8,30]. It was more likely to cause runoff and sediment in the Peijiamaogou watershed under rainfall type A when the erosion-prone area was covered with higher rainfall intensity. Hence, the thresholds of CAP for P under rainfall type A were more smaller than those under rainfall type B (Table 6). The results can provide reference for water erosion prediction at the subwatershed and watershed scales.

4.2. The Thresholds of Sediment-Generating Rainfall across Different Spatial Scales

The scale-dependency of the soil erosion and sediment transportation in the Loess Plateau region has been demonstrated by previous studies [24,25,40,46]. Within subwatersheds, sediment generated from the hillslope may deposit at the sediment sinks at the foot of hillslopes or store in valley bottoms and channel [5,47,48]. Consequently, in the subwatershed, more runoff which was produced by rainfall events with higher rainfall intensity was needed to transport the sediment produced from the hillslope to the outlets of the subwatersheds. Hence, I_{30} thresholds increased as the spatial scale transformed the hillslope into the subwatershed (Table 3).

The previously described laws were not suitable for the spatial scale of the watershed. Liu et al. [49] found that the rainfall characteristics in the watersheds with an area larger than 5 km^2 were characterized by high spatial heterogeneity and positively correlated with the area of the watersheds [34]. As an example, the mean I_{30} of a rainfall event in the Peijiamaogou watershed happened in July 2006, was only 0.21 mm min^{-1}, yet two rainfall stations in the Peijiamaogou watershed showed I_{30} of 0.70 and 0.72 mm min^{-1}. In some rainfall events with lower mean rainfall intensities, part of the area of the watersheds may be covered by high rainfall intensity far higher than the thresholds of the subwatersheds. Consequently, that part of the area may serve as sediment source area in the runoff events. Rainfall with high intensity caused runoff in sediment source areas, and the runoff generated by intense rainfall was high enough to transport the sediment produced from the subwatersheds or stored in channel to the outlets of the outer watersheds [47]. Namely, the sediment sinks in events with small rainfall intensity may be transformed to sediment sources in these circumstances. Additionally, the watersheds would generate sediment more easily if the areas covered by high rainfall intensity were close to outlets of watersheds. Thus, the I_{30} threshold of the watershed (Peijiamaogou) was not only smaller than those of the subwatersheds, but also relatively small as opposed to those of runoff plots (Table 3). This also implies that the spatial heterogeneity of rainfall characteristics in larger watersheds should be taken into consideration in studies of runoff and sediment generation of watersheds in the Loess Plateau region [27].

4.3. The Index Selection for Thresholds of Sediment-Generating Rainfall

Generally, the I_{30} should be recommended as rainfall index for the thresholds of sediment-generating rainfall to effectively reduce the considerable work of calculating the rainfall erosivity from hillslope to watershed scales in the loess hilly areas. Among rainfall indexes for the thresholds of sediment-generating rainfall, the I_{30} had the least MIs of thresholds, including the thresholds across different spatial scales and the CAP (Figure 2, Table 3). This finding proves the result reported by Xie et al. [8] at the hillslope and subwatershed scales. Besides, the other maximum rainfall intensities and recombination indexes can be supplementary thresholds. However, the P was not recommended as the rainfall index for the thresholds of sediment-generating rainfall. Thresholds of P exhibited highest MIs among all rainfall indexes, with average values of 13.1% (Figure 2). Additionally, the N_{up}/N_t of P also showed higher than those of other rainfall indexes and the values of N_{up}/N_t were much higher than that of N_{dn}/N_t. These results indicate that taking the rainfall amount as thresholds of sediment-generating rainfall would underestimate the values of threshold sediment-generating rainfall and lead to superfluous work of calculating rainfall erosivity (Figure 2). This phenomenon also indicates that rainfall events with higher rainfall amount and smaller maximum 30-min intensity may not cause sediment across different spatial scales, and I_{30} is a suitable factor predicting the soil loss [34,35].

In watersheds, the mean rainfall indexes (P, I_{30}, PI_{30}) were difficult to represent the rainfall characteristics explicitly and roundly under a rainfall event [34,49,50]. Accordingly, thresholds of mean rainfall indexes also led to an under-representation of the spatial distribution of critical sediment-generating rainfall in larger watersheds. Thus, the thresholds of CAP (covering area proportion) that we proposed can be used at both subwatershed and watershed scales. For instance, thresholds of CAP for P in the Qiaogou subwatershed and the Peijiamaogou watershed were 50.5% and 31.0%, respectively. These thresholds meant that the percent of area with rainfall amount higher than their mean thresholds (15.6 mm in Qiaogou and 15.9 mm in Peijiamaogou) to the total area of the subwatershed and the watershed were 50.5% and 31.0%, respectively. The thresholds for CAP could distinguish effectively the rainfall events which generated sediment or not in the subwatersheds and the watersheds well, because the MIs of thresholds for CAP were smaller (Figure 2, Table 4).

Other factors, such as rainfall during the early stage and underlying conditions (land use types, agrotype, and topography), could impact the thresholds of sediment-generating rainfall [11,13,17]. As has been documented, the soil moisture content before the rainfall has an influence on the runoff and soil loss [51–53]. Hence, antecedent rainfall could also be considered in the process of soil erosion and the obtainment of the thresholds for sediment-generating rainfall. However, the effects of other factors have not been included in this study because of insufficient data of antecedent rainfall and underlying conditions. Also, the current study obtained the thresholds of sediment-generating rainfall across different spatial scales, while the temporal scales of rainfall thresholds have not been studied in our research. In sum, the role of other factors and temporal scales on the thresholds should be studied further in future researches.

5. Conclusions

In the present study, thresholds of sediment-generating rainfall across different spatial scales under different rainfall types were determined based on observations of rainfall and sediment data of twelve instrumented nested landscape units from 1990 to 2010. I30 was deemed to be most suitable among all thresholds of rainfall indexes because of the smaller MIs, whereas P was not recommended as thresholds of sediment-generating rainfall due to higher MIs. In addition, thresholds of CAP for P and I30 were 50.5% and 47.6% at the subwatershed scale, and 31.0% and 30.3% at the watershed scale, respectively. In general, all thresholds (P, I30, I60 and PI30, PI60) of the subwatershed scale were nearly higher than those of hillslope scale. Regarding the watershed scale, the threshold of I30 was smaller in contrast with the other scales. The thresholds of sediment-generating rainfall were inconsistent under different rainfall types. The thresholds of I30 under rainfall type B were much higher than those under rainfall type A at the hillslope scale and smaller than those under rainfall type A at the subwatershed and watershed scales.

The results of thresholds for sediment-generating rainfall across different spatial scales cannot only be applied to the Loess Plateau, but also be extrapolated to other loess hilly areas with similar climatic conditions, soil characteristics, and geomorphologic landscapes worldwide. This study can provide a reference for calculating rainfall erosivity and predicting soil erosion and sediment yield across different spatial scales, as well as sideways verification of the theory of spatial scale effect of soil erosion and sediment yield.

Author Contributions: Conceptualization, J.J.; Formal analysis, Y.L.; Funding acquisition, J.J.; Methodology, Y.L.; Resources, W.D. and W.C.; Writing—original draft, Y.L.; Writing—review and editing, Y.L. and J.J.

Funding: This work was supported by the National Key Research and Development Program of China (No. 2016YFC0501604), the National Natural Science Foundation of China (no. 41771319), and the project of institute of soil and water conservation (CAS and MWC) on the comprehensive survey of soil and water conservation under "726" extreme rainstorm in Wuding river basin.

Acknowledgments: The authors thank the Suide station of the Yellow River Water Conservancy Commission (YRWCC) for monitoring the rainfall and sediment data. The authors also thank their colleagues Meng Kou, Yixian Chen, and Bingzhe Tang for reviewing this manuscript.

Conflicts of Interest: The authors declare no conflict of interest.

References

1. Lal, R. Soil erosion and the global carbon budget. *Environ. Int.* **2003**, *29*, 437–450. [CrossRef]
2. Bakker, M.M.; Govers, G.; Rounsevell, M.D.A. The crop productivity–erosion relationship: An analysis based on experimental work. *Catena* **2004**, *57*, 55–76. [CrossRef]
3. Rajan, K. Soil organic carbon–the most reliable indicator for monitoring land degradation by soil erosion. *Curr. Sci.* **2010**, *99*, 823–827. [CrossRef]
4. Zhao, J.; Van Oost, K.; Chen, L.; Govers, G. Moderate topsoil erosion rates constrain the magnitude of the erosion-induced carbon sink and agricultural productivity losses on the Chinese Loess Plateau. *Biogeosciences* **2015**, *12*, 14981–15010. [CrossRef]
5. García-Ruiz, J.M.; Beguería, S.; Lana-Renault, N.; Nadal-Romero, E.; Cerdà, A. Ongoing and Emerging Questions in Water Erosion Studies. *Land Degrad. Dev.* **2017**, *28*, 5–21. [CrossRef]
6. Valero-Garcés, B.L.; Navas, A.; Machín, J.; Walling, D. Sediment Sources and Siltation in Mountain Reservoirs: A Case Study from the Central Spanish Pyrenees. *Geomorphology* **1999**, *28*, 23–41. [CrossRef]
7. Wischmeier, W.H.; Smith, D.D. Rainfall energy and its relationship to soil loss. *Eos Trans. Am. Geophys. Union* **1958**, *39*, 285–291. [CrossRef]
8. Xie, Y.; Liu, B.; Nearing, M.A. Practical thresholds for separating erosive and non-erosive storms. *Trans. ASAE* **2002**, *45*, 1843–1847. [CrossRef]
9. Fang, N.F.; Wang, L.; Shi, Z.H. Runoff and soil erosion of field plots in a subtropical mountainous region of China. *J. Hydrol.* **2017**, *552*, 387–395. [CrossRef]
10. Todisco, F. The internal structure of erosive and non-erosive storm events for interpretation of erosive processes and rainfall simulation. *J. Hydrol.* **2014**, *519*, 3651–3663. [CrossRef]
11. Xia, L.; Song, X.Y.; Fu, N.; Li, H.Y.; Li, Y.L. Threshold standard of erosive rainfall under different underlying surface conditions in the loess plateau Gully Region of East Gansu, China. *Adv. Water Sci.* **2018**, *29*, 828–838. (In Chinese) [CrossRef]
12. Wischmeier, W.H.; Smith, D.D. Predicting Rainfall Erosion Losses: A Guide for Conservation Planning. In *Agriculture Handbook*; United States Department of Agriculture: Washington, DC, USA, 1978; p. 537.

13. Wang, B.W.; Fang, S.W.; Song, Y.J.; Yang, J. Research for standard of erosive rainfall on Quaternary Red Soil area in north of Jiangxi province in China. *Trans. Chin. Soc. Agric. Eng.* **2013**, *29*, 100–106. (In Chinese) [CrossRef]
14. Wang, W.Z. Study on the relations between rainfall characteristics and loss of soil in loess region. *Bull. Soil Water Conserv.* **1984**, 58–63. (In Chinese) [CrossRef]
15. Yu, B.; Rosewell, C. An assessment of a daily rainfall erosivity model for new south wales. *Aust. J. Soil Res.* **1996**, *34*, 139–152. [CrossRef]
16. Renard, K.G.; Foster, G.R.; Weesies, G.A.; McCool, D.K.; Yoder, D.C. Predicting soil erosion by water: A guide to conservation planning with the revised universal soil loss equation (RUSLE). In *Agricultural Handbook*; United States Department of Agriculture: Washington, DC, USA, 1997; p. 703.
17. Zhou, D.P.; Xiong, M.B.; Lin, L.J.; Wang, H.H. Influence of slope gradient on erosive values in slope cropland with purple soil. *Bull. Soil Water Conserv.* **2009**, *29*, 159–162, 167. [CrossRef]
18. Cantón, Y.; Solé-Benet, A.; Vente, J.D.; Boix-Fayos, C.; Calvo-Cases, A.; Asensio, C.; Puigdefábregas, J. A review of runoff generation and soil erosion across scales in semiarid south-eastern Spain. *J. Arid Environ.* **2011**, *75*, 1254–1261. [CrossRef]
19. Fang, H.Y.; Chen, H.; Cai, Q.G.; Li, Q.Y. Scale effect on sediment yield from sloping surfaces to basins in hilly loess region on the loess plateau in china. *Environ. Geol.* **2007**, *52*, 753–760. [CrossRef]
20. Lei, A.L.; Tang, K.L. Significance and Character of Conception of Soil Erosion Chain. *J. Soil Water Conserv.* **2000**, *14*, 79–83. (In Chinese) [CrossRef]
21. Matmon, A.; Bierman, P.R.; Larsen, J.; Southworth, S.; Pavich, M.; Caffee, M. Temporally and spatially uniform rates of erosion in the southern appalachian great smoky mountains. *Geology* **2003**, *31*, 155. [CrossRef]
22. Tooth, S. Process, form and change in dryland rivers: A review of recent research. *Earth-Sci. Rev.* **2000**, *51*, 67–107. [CrossRef]
23. Verstraeten, G.; Prosser, I.P.; Fogarty, P. Predicting the spatial patterns of hillslope sediment delivery to river channels in the Murrumbidgee catchment, Australia. *J. Hydrol.* **2007**, *334*, 440–454. [CrossRef]
24. Zheng, M.G.; Qin, F.; Sun, L.Y.; Qi, D.; Cai, Q.G. Spatial scale effects on sediment concentration in runoff during flood events for hilly areas of the loess plateau, China. *Earth Surf. Process. Landf.* **2011**, *36*, 1499–1509. [CrossRef]
25. Zheng, M.G.; Yang, J.S.; Qi, D.L.; Sun, L.Y.; Cai, Q.G. Flow-sediment relationship as functions of spatial and temporal scales in hilly areas of the Chinese loess plateau. *Catena* **2012**, *98*, 29–40. [CrossRef]
26. Liang, Y.; Jiao, J.Y. Analysis on rainfall standards while sediment occurring in small watersheds on the Loess Plateau. *Sci. Soil Water Conserv.* **2019**, *17*, 8–14. [CrossRef]
27. Wang, L.L.; Yao, W.Y.; Wang, W.L.; Yang, E.; Chen, L.; Zhang, P. Sediment transport capacity and flow-sediment relationship in different topographical units of different spatial scales in hilly loess region. *Trans. Chin. Soc. Agric. Eng.* **2015**, *31*, 120–126. (In Chinese) [CrossRef]
28. Zhao, B.H.; Li, Z.B.; Li, P.; Xiao, L.; Chang, E.H.; Zhang, Y.; Gao, B. Effects of ecological construction on transformation of different water bodies in typical watershed on loess plateau. *Trans. Chin. Soc. Agric. Eng.* **2017**, *33*, 179–187. (In Chinese) [CrossRef]
29. Liu, B.Y.; Nearing, M.A.; Shi, P.J.; Jia, Z.W. Slope Length Effects on Soil Loss for Steep Slopes. *Soil Sci. Soc. Am. J.* **2000**, *64*, 1759. [CrossRef]
30. Gao, H.D.; Li, Z.B.; Jia, L.L.; Li, P. Estimation of evapotranspirations from watersheds under different water and soil conservation measures using SEBAL model—A case study of Jiuyuangou and Peijiamao. *Acta Pedol. Sin.* **2012**, *49*, 260–268. (In Chinese)
31. Wang, L.L. *Runoff-Sediment Coupling Mechanism of Different Geomorphic Unit in the Loess Hilly-Gully Region Doctor*; Northwest A&F University: Yangling, China, 2017. (In Chinese)
32. Zheng, M.G.; Cheng, W.M. Determination of erosive events in the Chinese Loess Plateau using the runoff threshold. *J. Soils Sediments* **2017**, *17*, 1182–1190. [CrossRef]
33. Huff, F.A. Time distribution of rainfall in heavy storms. *Water Resour. Res.* **1967**, *3*, 1007–1019. [CrossRef]
34. Wang, W.Z.; Jiao, J.Y. *Rainfall and Erosion Sediment Yield and Sediment Reduction of Soil and Water Conservation in the Loess Plateau*; Science China Press: Beijing, China, 1996. (In Chinese)
35. Zheng, M.G.; Chen, X.A.; Magar, V. Statistical determination of rainfall-runoff erosivity indices for single storms in the chinese loess plateau. *PLoS ONE* **2015**, *10*. [CrossRef] [PubMed]

36. Bi, C.X. Study on Watershed Sediment Yield Rainfall and Contributions of the Watershed Sediment Yield Rainfall to Runoff and Sediment in Huangfuchuan River Basin. Master's Thesis, Chinese Academy of Sciences, Yangling, China, 2013. (In Chinese).
37. Zheng, M.G. Scale independence and spatial uniformity of specific sediment yield in loess areas of the wuding river basin, northwest china. *Land Degrad. Dev.* **2017**, *28*, 1450–1462. [CrossRef]
38. Chen, H.; Zhang, X.P.; Abla, M.; Lü, D.; Yan, R.; Ren, Q.F.; Ren, Z.Y.; Yang, Y.H.; Zhao, W.H.; Li, P.F.; et al. Effects of vegetation and rainfall types on surface runoff and soil erosion on steep slopes on the loess plateau, China. *Catena* **2018**, *170*, 141–149. [CrossRef]
39. Jiao, J.Y.; Wang, W.Z.; Hao, X.P. Precipitation and erosion characteristics of rain-storm in different pattern on Loess Plateau. *J Arid Land Resour. Environ.* **1999**, *13*, 38–42. (In Chinese) [CrossRef]
40. Fang, H.Y.; Cai, Q.G.; Chen, H.; Li, Q.Y. Effect of Rainfall Regime and Slope on Runoff in a Gullied Loess Region on the Loess Plateau in China. *Environ. Manag.* **2008**, *42*, 402–411. [CrossRef]
41. Bochet, E.; Poesen, J.; Rubio, J.L. Runoff and soil loss under individual plants of a semi-arid mediterranean shrubland. *Earth Surf. Process. Landf.* **2006**, *31*, 536–549. [CrossRef]
42. Esteves, M.; Lapetite, J.M. A multi-scale approach of runoff generation in a sahelian gully catchment: A case study in niger. *Catena* **2003**, *50*, 255–271. [CrossRef]
43. De Roo, A.P.J.; Riezebos, H.T.H. Infiltration experiments on loess soils and their implications for modeling surface runoff and soil erosion. *Catena* **1992**, *19*, 221–239. [CrossRef]
44. Zhang, Q.W.; Wang, Z.L.; Wu, B.; Shen, N.; Liu, J.E. Identifying sediment transport capacity of raindrop-impacted overland flow within transport-limited system of interrill erosion processes on steep loess hillslopes of china. *Soil Tillage Res.* **2018**, *184*, 109–117. [CrossRef]
45. Wei, W.; Jia, F.Y.; Yang, L.; Chen, L.D.; Zhang, H.D.; Yu, Y. Effects of surficial condition and rainfall intensity on runoff in a loess hilly area, china. *J. Hydrol.* **2014**, *513*, 115–126. [CrossRef]
46. Zheng, M.G. A spatially invariant sediment rating curve and its temporal change following watershed management in the Chinese Loess Plateau. *Sci. Total Environ.* **2018**, *630*, 1453–1463. [CrossRef] [PubMed]
47. Buendia, C.; Vericat, D.; Batalla, R.J.; Gibbins, C.N. Temporal Dynamics of Sediment Transport and Transient In-channel Storage in a Highly Erodible Catchment. *Land Degrad. Dev.* **2016**, *27*, 1045–1063. [CrossRef]
48. Nadal-Romero, E.; Petrlic, K.; Verachtert, E.; Bochet, E.; Poesen, J. Effects of slope angle and aspect on plant cover and species richness in a humid Mediterranean badland. *Earth Surf. Process. Landf.* **2014**, *39*, 1705–1716. [CrossRef]
49. Liu, Y.B. Rainfall Erosivity Modeling of Small Watershed. Ph.D. Thesis, Institute of Soil and Water Conservation Chinese Academy of Sciences, Yangling, China, 1990. (In Chinese).
50. Bull, L.J.; Kirkby, M.J.; Shannon, J.; Hooke, J.M. The impact of rainstorms on floods in ephemeral channels in southeast Spain. *Catena* **2000**, *38*, 191–209. [CrossRef]
51. Nortcliff, S.; Ross, S.M.; Thornes, J.B. Soil moisture, runoff and sediment yield from differentially cleared tropical rainforest plots. In *Vegetation and Erosion: Processes and Environ*; John Wiley and Sons Ltd.: Chichester, UK, 1990; pp. 419–436.
52. Scipal, K.; Scheffler, C.; Wagner, W. Soil moisture-runoff relation at the catchment scale as observed with coarse resolution microwave remote sensing. *Hydrol. Earth Syst. Sci.* **2005**, *2*, 417–448. [CrossRef]
53. Zhou, J.; Fu, B.J.; Gao, G.Y.; Lu, Y.H.; Liu, Y.; Lu, N.; Wang, S. Effects of precipitation and restoration vegetation on soil erosion in a semi-arid environment in the Loess Plateau, China. *Catena* **2016**, *137*, 1–11. [CrossRef]